

Farey Sequences and the Planar Euclidean Medial Axis Test Mask

Jérôme Hulin and Édouard Thiel *

Laboratoire d'Informatique Fondamentale de Marseille (LIF, UMR 6166),
Aix-Marseille Université,
163 Avenue de Luminy, Case 901, 13288 Marseille cedex 9, France.

e-mail: {Jerome.Hulin, Edouard.Thiel}@lif.univ-mrs.fr
url: <http://www.lif.univ-mrs.fr/~thiel/>

Abstract. The Euclidean test mask $\mathcal{T}(r)$ is the minimum neighbourhood sufficient to detect the Euclidean Medial Axis of any discrete shape whose inner radius does not exceed r . We establish a link between $\mathcal{T}(r)$ and the well-known Farey sequences, which allows us to propose two new algorithms. The first one computes $\mathcal{T}(r)$ in time $\mathcal{O}(r^4)$ and space $\mathcal{O}(r^2)$. The second one computes for any vector \vec{v} the smallest r for which $\vec{v} \in \mathcal{T}(r)$, in time $\mathcal{O}(r^3)$ and constant space.

Keywords: medial axis, Farey sequence, Euclidean distance.

1 Introduction

The Medial Axis is a geometrical tool, which is widely used in numerous fields of image analysis [1]. The basic idea is simple: consider a subset \mathcal{S} of a space E ; the medial axis MA of \mathcal{S} is the set of centres (and radii) of all maximal disks in \mathcal{S} . A disk D is maximal in \mathcal{S} if D is included in \mathcal{S} and if D is not included in any other disk included in \mathcal{S} . Thus $\text{MA}(\mathcal{S})$ is a covering of \mathcal{S} and so, the list of centres and radii of $\text{MA}(\mathcal{S})$ is a reversible coding, a key point in many applications.

Another important point of interest about MA is that detecting the centres of maximal disks can be very efficiently achieved using a distance transform of \mathcal{S} . The distance transform $\text{DT}(\mathcal{S})$ is a copy of \mathcal{S} where each point is labeled with its distance to the closest point of the background $E \setminus \mathcal{S}$. The geometric properties of MA, as well as the computation of DT, both depend on the distance function. The main distances used in discrete geometry are the Euclidean distance d_E [2], generally squared to get integer values in $E = \mathbb{Z}^n$, and the chamfer (or weighted) norms [3].

The general method to extract MA from DT, applicable to d_E and chamfer norms in \mathbb{Z}^n , is known as the LUT method [4, 5]. A precomputation [6, 7] gives a neighbourhood T and a look-up table LUT; then, to know if a point $p \in \mathcal{S}$ is a medial axis point, it is sufficient to check the neighbours $p + \vec{v}$ for all $\vec{v} \in T$ and

* Work supported in part by ANR grant BLAN06-1-138894 (projet OPTICOMB).

compare their DT values to the values stored in LUT. Lately, a fast algorithm using H-polytopes was proposed for 2D and 3D chamfer norms in [8, 9].

Instead of computing T , we may use $T = \mathbb{Z}^n$, but the MA extraction would be excessively long. On the other hand, if T too small, the MA extraction may choose non maximal disks. Therefore, we aim at computing a minimal T with respect to a class of shapes: Given a distance d in \mathbb{Z}^n , n fixed, and a radius r , we denote by $\mathcal{T}(r)$ the minimum test neighbourhood sufficient to extract the MA of all n -dimensional shapes whose inner radius are not greater than r .

Concerning the Euclidean distance, we have proved in [10] that in any dimension, $\mathcal{T}(r)$ is unique and tends to the set of visible vectors when r tends to infinity. We have recently tackled the search of arithmetical and geometrical properties concerning $\mathcal{T}(r)$ and the appearance radii of vectors in the 2-dimensional case. We have presented recent results concerning 5×5 chamfer norms in [11]; in this paper we present new properties in the Euclidean case.

When r grows, new vectors (that is to say, neighbours) are inserted from time to time in $\mathcal{T}(r)$. Given a vector \vec{v} , we denote by $r_{app}(\vec{v})$ the appearance radius of \vec{v} , that is, the smallest r for which $\vec{v} \in \mathcal{T}(r)$.

In order to incrementally find the new vectors of $\mathcal{T}(r)$, the method proposed in [6, 7] consists in checking, for every point p in a disk of radius r , disks inclusion relations in directions $p + \vec{v}$, for all $\vec{v} \in \mathcal{T}(r)$. In this paper, we show that it is sufficient to test the inclusion relations with two neighbours, instead of all the neighbours of $\mathcal{T}(r)$. These two points are indeed the neighbours of p in some Farey sequence [12].

This property has two consequences: first, the computation of $\mathcal{T}(r)$ can be sped up significantly. Second, these two points to test are independent from $\mathcal{T}(r)$, so we are able to compute the appearance radius $r_{app}(\vec{v})$ of any visible vector \vec{v} without computing \mathcal{T} up to $r_{app}(\vec{v})$.

In Section 2 we introduce the definitions which are used in Section 3, where we establish the link between Farey sequences and the appearance radii of visible vectors. Then we present the two algorithms in Sections 4 and 5. We conclude by observations and conjectures in Section 6.

2 Preliminaries

2.1 The discrete space \mathbb{Z}^n

Throughout the paper, we work in the discrete space \mathbb{Z}^n (we will at some point fix $n = 2$). We consider \mathbb{Z}^n both as an n -dimensional \mathbb{Z} -module (a discrete vector space) and as its associated affine space; and we write $\mathbb{Z}_*^n = \mathbb{Z}^n \setminus \{0\}$. We denote by (v_1, \dots, v_n) the Cartesian coordinates of a given vector \vec{v} . A vector $\vec{Op} \in \mathbb{Z}^n$ (or a point $p \in \mathbb{Z}^n$) is said to be *visible* if the line segment connecting O to p contains no other point of \mathbb{Z}^n , i.e., if the coordinates of p are coprime.

We call Σ^n the group of axial and diagonal symmetries in \mathbb{Z}^n about centre O . The cardinal of the group is $\#\Sigma^n = 2^n n!$ (which is 8, 48 and 384 for $n = 2, 3$ and 4). An n -dimensional *shape* \mathcal{S} is by definition a subset of \mathbb{Z}^n . A shape \mathcal{S} is

said to be *G-symmetrical* if for every $\sigma \in \Sigma^n$ we have $\sigma(\mathcal{S}) = \mathcal{S}$. The *generator* of a set $\mathcal{S} \subseteq \mathbb{Z}^n$ is $G(\mathcal{S}) = \{ (p_1, \dots, p_n) \in \mathcal{S} : 0 \leq p_n \leq p_{n-1} \leq \dots \leq p_1 \}$.

2.2 Balls and medial axis

Let d be a distance on \mathbb{Z}^n . The *ball* of centre $p \in \mathbb{Z}^n$ and radius $r \in \mathbb{R}$ is $\mathcal{B}(p, r) = \{ q \in \mathbb{Z}^n : d(p, q) \leq r \}$. To shorten notation, we let B_r stand for $\mathcal{B}(O, r)$. Since we consider discrete closed balls, any ball B has an infinite number of real radii in a left-closed interval $[r_1, r_2[$, with $r_1, r_2 \in \text{Im}(d)$. We define the *representable radius* of a given ball B to be the radius of B which belongs to $\text{Im}(d)$.

Let \mathcal{S} be a shape and $p \in \mathbb{Z}^n$. We define $I_p(\mathcal{S})$ to be the largest ball of centre p , included in \mathcal{S} (if $p \notin \mathcal{S}$, we have $I_p(\mathcal{S}) = \emptyset$). Analogously, we define $H_p(\mathcal{S})$ to be the smallest ball of centre p , which contains \mathcal{S} . We also define $\mathcal{R}_p(B)$ to be the representable radius of $H_p(B)$. See an example in Fig. 1. The *inner radius* of a given shape \mathcal{S} , denoted by $\text{rad}(\mathcal{S})$, is the representable radius of a largest ball included in \mathcal{S} . We denote by $\text{CS}^n(r)$ the class of all n -dimensional shapes whose inner radius are less than or equal to r . A ball included in a shape \mathcal{S} is said to be *maximal* in \mathcal{S} if it is not included in any other ball included in \mathcal{S} . The *Medial Axis* (MA) of a shape \mathcal{S} is the set of centres (and radii) of all maximal balls of \mathcal{S} :

$$p \in \text{MA}(\mathcal{S}) \Leftrightarrow p \in \mathcal{S} \text{ and } \forall q \in \mathcal{S} \setminus \{p\}, I_p(\mathcal{S}) \not\subseteq I_q(\mathcal{S}). \quad (1)$$

Finally, if a point $q \in \mathcal{S}$ satisfies $I_p(\mathcal{S}) \subseteq I_q(\mathcal{S})$, we say that q *forbids* p from $\text{MA}(\mathcal{S})$, see Fig. 3.

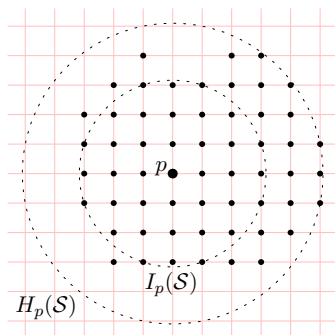


Fig. 1. $H_p(\mathcal{S})$ and $I_p(\mathcal{S})$ for a shape \mathcal{S} (\mathcal{S} is represented by bullets).

8	5	4	5	8
5	2	1	2	5
4	1	O	1	4
5	2	1	2	5
8	5	4	5	8

Fig. 2. Balls of squared Euclidean radii 1 (shaded) and 2 (delimited by the thick line). Values indicate the distance to O .

2.3 The medial axis test mask \mathcal{T}

For the coherence of what follows, we assume d is a translation invariant distance. We define the *test mask* $\mathcal{T}(r)$ to be the minimum neighbourhood sufficient to

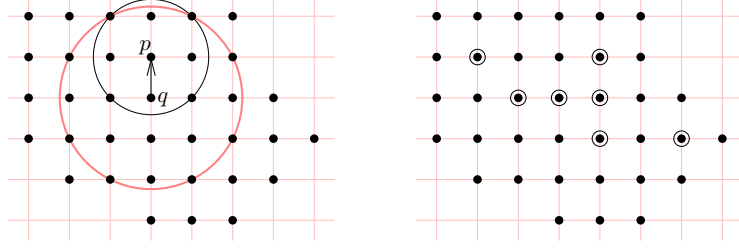


Fig. 3. Left: A shape \mathcal{S} (bullets). Since $I_p(\mathcal{S}) \subseteq I_q(\mathcal{S})$, the point q forbids p from $\text{MA}(\mathcal{S})$. Right: the medial axis of \mathcal{S} (circled points).

detect locally, for all \mathcal{S} in $\text{CS}^n(r)$ and all $p \in \mathcal{S}$, if p is a point of $\text{MA}(\mathcal{S})$:

$$\begin{cases} \forall \mathcal{S} \in \text{CS}^n(r), \forall p \in \mathcal{S}, \left(p \notin \text{MA}(\mathcal{S}) \Rightarrow \exists \vec{v} \in \mathcal{T}(r), I_p(\mathcal{S}) \subseteq I_{p-\vec{v}}(\mathcal{S}) \right); \\ \mathcal{T}(r) \text{ has minimum cardinality.} \end{cases} \quad (2)$$

We have shown the unicity of $\mathcal{T}(r)$ for all $r \geq 0$ in [10]. As a corollary, if the considered distance is G-symmetrical, then so is $\mathcal{T}(r)$. Therefore, by abuse of notation we write $\mathcal{T}(r)$ instead of $\text{G}(\mathcal{T}(r))$. Finally, the *appearance radius* $r_{app}(\vec{v})$ of a given vector \vec{v} is the smallest radius r for which $\vec{v} \in \mathcal{T}(r)$.

Once we have a pre-computed test mask $\mathcal{T}(r)$, it is quite straightforward to compute the MA of a given $\mathcal{S} \in \text{CS}^n(r)$: first, compute for each $p \in \mathcal{S}$, the ball $I_p(\mathcal{S})$. $\text{DT}(p)$ is the distance from p to $\mathbb{Z}^n \setminus \mathcal{S}$, so $I_p(\mathcal{S})$ is equal to the open ball of radius $\text{DT}(p)$. Second, test for each point $p \in \mathcal{S}$ whether $I_p(\mathcal{S})$ is included in some $I_{p-\vec{v}}(\mathcal{S})$, with $\vec{v} \in \mathcal{T}(r)$.

Actually, the hard part consists in computing $\mathcal{T}(r)$, as we will see. According to (2), finding the appearance radius of a given vector \vec{v} consists in solving the following **keyhole problem**: Given a vector \vec{v} , find the smallest positive r s.t. there is no ball B satisfying $I_{O+\vec{v}}(B_r) \subsetneq B \subsetneq B_r$. The term *key* refers to the ball B that we are trying to insert between B_r and $I_{O+\vec{v}}(B_r)$.

It is easy to check that the above problem is equivalent to finding the smallest positive $\mathcal{R}_{O+\vec{v}}(B_r)$ s.t. there is no ball B satisfying $B_r \subsetneq B \subsetneq H_{O+\vec{v}}(B_r)$. We would like to test as few balls (keys) B as possible when solving the keyhole problem:

Definition 1 (Set of keys) *Given a vector $\vec{v} \in \mathbb{Z}^n$, a set A is called a set of keys of \vec{v} iff A is a neighbourhood sufficient to solve the keyhole problem with parameter \vec{v} . Precisely, A is a set of keys of \vec{v} iff*

$$\vec{0}, \vec{v} \notin A \text{ and } \forall r < r_{app}(\vec{v}), \exists \vec{u} \in A \text{ s.t. } H_{O-\vec{u}}(B_r) \subseteq H_{O-\vec{v}}(B_r).$$

We aim at finding a set of keys of \vec{v} having minimal cardinality. To do so, we define a domination relation as follows:

Definition 2 (\vec{v} -Domination) We say that a vector \vec{u} is \vec{v} -dominated by a vector \vec{u}' ($\vec{u} \prec_{\vec{v}} \vec{u}'$ for short) iff

$$\forall r \geq 0, \left(H_{O-\vec{u}'}(B_r) \not\subseteq H_{O-\vec{v}}(B_r) \Rightarrow H_{O-\vec{u}}(B_r) \not\subseteq H_{O-\vec{v}}(B_r) \right).$$

Thus, if $\vec{u} \prec_{\vec{v}} \vec{u}'$, then \vec{u} can be replaced by \vec{u}' in any set of keys of \vec{v} . Notice that $\prec_{\vec{v}}$ is not a total order, however it is clearly reflexive and transitive.

2.4 Farey Sequences

Let k be a positive integer. The *Farey sequence* of order k is the sequence of all irreducible fractions between 0 and 1, whose denominators do not exceed k , arranged in increasing order. For example, the Farey sequence of order 5 is

$$F_5 = \left\{ \frac{0}{1}, \frac{1}{5}, \frac{1}{4}, \frac{1}{3}, \frac{2}{5}, \frac{1}{2}, \frac{3}{5}, \frac{2}{3}, \frac{3}{4}, \frac{4}{5}, \frac{1}{1} \right\}.$$

Let $0 < \frac{a}{b} < 1$ be an irreducible fraction. We call *predecessor* of $\frac{a}{b}$ the term which precedes $\frac{a}{b}$ in F_b ; we denote it by $\text{pred}(\frac{a}{b})$. Similarly, the *successor* of $\frac{a}{b}$, denoted by $\text{succ}(\frac{a}{b})$, is the term which follows $\frac{a}{b}$ in F_b . For example, the predecessor and the successor of $\frac{3}{4}$ are respectively $\frac{2}{3}$ and $\frac{1}{1}$. Cauchy proved that if $\frac{a}{b}$ and $\frac{c}{d}$ are two consecutive terms in some Farey sequence, then $bc - ad = 1$ (see [12] for details). Conversely, if $0 \leq \frac{a}{b} < \frac{c}{d} \leq 1$ are two irreducible fractions satisfying $bc - ad = 1$, then there is a Farey sequence in which $\frac{a}{b}$ and $\frac{c}{d}$ are neighbours. As a corollary, if $\frac{a}{b}, \frac{c}{f}, \frac{c}{d}$ are three consecutive terms in a Farey sequence, then $\frac{c}{f}$ is the *mediant* of $\frac{a}{b}$ and $\frac{c}{d}$, that is to say $\frac{c}{f} = \frac{a+c}{b+d}$. For instance $\frac{1}{4}, \frac{1}{3}, \frac{2}{5}$ are three consecutive terms in F_5 , so $\frac{1}{3} = \frac{1+2}{4+5}$.

In this paper, we will use a geometric interpretation of Farey sequences: each irreducible fraction $0 \leq \frac{y}{x} \leq 1$ can be associated with a visible point p (or a vector \vec{Op}) in $G(\mathbb{Z}^2)$, with coordinates (x, y) . By abuse of notation, we may write $p \in F_k$ or $\vec{Op} \in F_k$ if $\frac{y}{x}$ belongs to the Farey sequence F_k . Accordingly, the Farey sequence of order k is the sequence of all visible vectors of $G(\mathbb{Z}^2)$ whose abscissas do not exceed k , arranged counterclockwise from the x-axis. As an example, the points of F_6 are depicted in Fig. 4.

Let \vec{u} and \vec{v} be two consecutive vectors in some Farey sequence. Since $|u_1v_2 - u_2v_1| = 1$, the set $\{\vec{u}, \vec{v}\}$ is a basis of \mathbb{Z}^2 . Moreover, the triangle $(O, O + \vec{u}, O + \vec{v})$ has area $1/2$, and it contains only three lattice points — its vertices. Also, let \vec{w} be a visible vector whose predecessor and successor are respectively denoted by \vec{u} and \vec{v} . Since \vec{w} is the mediant of \vec{u} and \vec{v} , we have $\vec{w} = \vec{u} + \vec{v}$ (see Fig. 5 for an example).

3 Farey sequences and \vec{v} -domination

From now on, we use the squared Euclidean distance d_E^2 in the space \mathbb{Z}^2 . The variable $R \in \mathbb{N}$ will always denote a squared Euclidean radius. Also, we

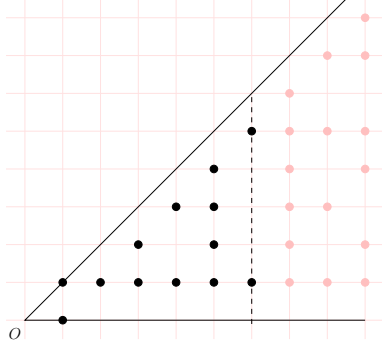


Fig. 4. Points of the Farey sequence of order 6 (in black) among the visible points in $G(\mathbb{Z}^2)$ (in grey).

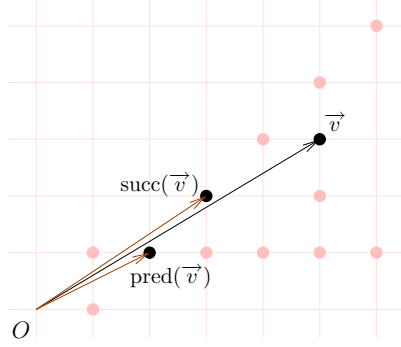


Fig. 5. The predecessor and the successor of $(5, 3)$ are respectively $(2, 1)$ and $(3, 2)$.

write $R_{app}(\vec{v})$ for the squared Euclidean appearance radius of \vec{v} : $R_{app}(\vec{v}) = r_{app}^2(\vec{v})$. For abbreviation, we write pq instead of $d_E^2(p, q)$. Nevertheless, since d_E^2 is not a norm, the standard notation $\|\vec{v}\|$ will denote the Euclidean norm of \vec{v} . Notice that d_E^2 is not even a metric, however it is important to point out that the medial axis with d_E and d_E^2 are identical, since these two distances yields the same set of balls.

Throughout this section, \vec{v} denotes a visible vector in $G(\mathbb{Z}^2)$ different from $(1, 0)$ and $(1, 1)$. We set $p = O + \vec{v}$, and we denote by q and q' (respectively) the predecessor and the successor of p . Also, the points $p'(p_1, 0)$ and $p''(p_1, p_1)$ are the points with same abscissa as p and minimal (resp. maximal) ordinate in $G(\mathbb{Z}^2)$, see Fig. 6.

Lemma 1 *If t is a lattice point inside the triangle (Opp') (different from O and p) then q belongs to the triangle (Opt) . Besides, if t is a lattice point in the triangle (Opp'') (different from O and p) then q' belongs to the triangle (Opt) .*

Proof. We prove the Lemma in the case where $t \in (Opp')$. Since q is the predecessor of p , there is no vector in the cone $\vec{Oq}\mathbb{N} + \vec{Op}\mathbb{N}$ and whose abscissa is not greater than that of p . Suppose that q is not inside the triangle (Opt) ; the vector \vec{pt} must belong to the cone $\vec{pq}\mathbb{N} + \vec{pO}\mathbb{N}$, see Fig. 6. The point p is the median of q and q' so $\vec{Oq}' = \vec{qp}$ (and $\vec{Oq} = \vec{q'p}$). By symmetry, we deduce that \vec{tp} belongs to the cone $\vec{Op}\mathbb{N} + \vec{Oq'}\mathbb{N}$; furthermore its abscissa is not greater than that of \vec{Op} . It follows that there is a point between p and q' in the Farey sequence of order p_1 , which contradicts our assumption $q' = \text{succ}(p)$.

By symmetry, the same reasoning applies to the case where $t \in (Opp'')$. \square

The preceding Lemma states that all lattice points in the triangle $(Op'p'')$ belong to the shaded area drawn in Fig. 7 (with the exception of O and p). This

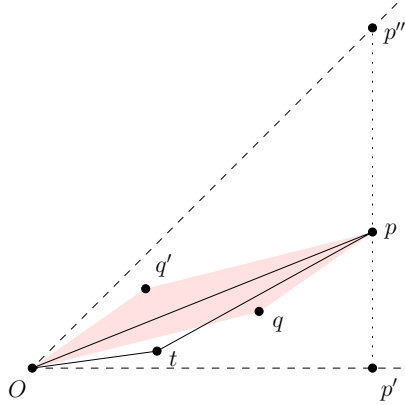


Fig. 6. Impossible configuration for the proof of Lemma 1. A visible point p , its predecessor q and successor q' (the shaded parallelogram has area 1 and contains only 4 lattice points — its vertices). For the sake of clarity, the angle \widehat{Oqp} is exaggerated.

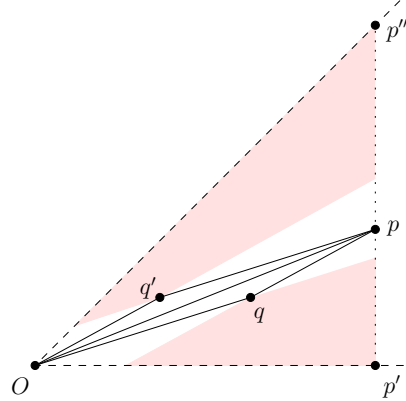


Fig. 7. The shaded areas (together with their boundaries) contain all the lattice points within the triangle $(Op'p'')$, with the exception of O and p .

geometrical property allows to establish \vec{v} -domination relations between points of $(Op'p'')$:

Lemma 2 *Every lattice point inside the triangle (Opp') is \vec{v} -dominated by q . Besides, every lattice point inside the triangle (Opp'') is \vec{v} -dominated by q' .*

Proof. We examine the case of a point $t \in (Opp'')$. Lemma 1 claims that $q' \in (Opt)$, i.e., t belongs to the upper shaded area in Fig. 7. Now, let B be a ball of centre O . According to Def. 2, it remains to prove that $H_{q'}(B) \not\subseteq H_p(B)$ implies $H_t(B) \not\subseteq H_p(B)$. Actually, it turns out that any point z in $H_{q'}(B) \setminus H_p(B)$ also belongs to $H_t(B)$, as we will see. Let x be a point of the ball B which maximizes the distance to q' , as illustrated in Fig. 8, left. We now need to establish three inequalities:

- By definition of x , the representable radius of $H_{q'}(B)$ is $q'x$. Moreover, $z \in H_{q'}(B)$, thus $q'z \leq q'x$.
- The point x belongs to B , unlike z (since $z \notin H_p(B)$ and $B \subseteq H_p(B)$). Accordingly, $Ox \leq Oz$.
- x belongs to $H_p(B)$ (because $x \in B$), but z does not, so $px \leq pz$.

These three inequalities give information about the position of O , p and q' with respect to the perpendicular bisector of the line segment $[xz]$: the points O and p lie on one side, while q' lies on the other, see Fig. 8, right. Moreover, q' is inside (Opt) , so t must lie on the same side of the bisector as q' . It follows that t is closer to z than x . However x belongs to $H_t(B)$, therefore z also belongs to $H_t(B)$, which is the desired conclusion.

Again, similar arguments apply in the case $t \in (Opp')$, to show $t \preceq_{\vec{v}} q$. \square

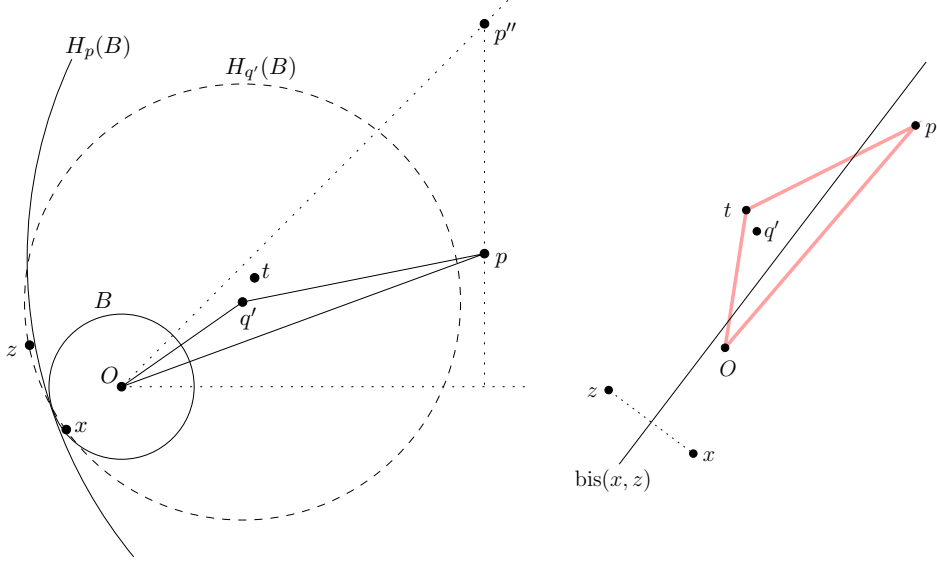


Fig. 8. Illustration for the proof of Lemma 2. Left: a point p and its successor q' . If for a ball B of centre O there is a point $z \in H_{q'}(B) \setminus H_p(B)$, then $z \in H_t(B)$. Right: position of the points O, p, q' and t with respect to the perpendicular bisector of $[xz]$.

We have shown in [10] that the set $\diamond \vec{v} = \{\vec{u} \in G(\mathbb{Z}_*^n) : \vec{v} - \vec{u} \in G(\mathbb{Z}_*^n)\}$ (roughly, a parallelogram) is a set of keys of any visible vector \vec{v} in $G(\mathbb{Z}^n)$. The set $\diamond \vec{v}$ is included in the triangle $(Op'p'')$, so Lemma 2 shows that any vector in $\diamond \vec{v}$ is \vec{v} -dominated either by $\text{pred}(\vec{v})$, or by $\text{succ}(\vec{v})$. We have thus proved:

Theorem 1 *Let \vec{v} be a visible vector in $G(\mathbb{Z}^2)$, different from $(1, 0)$ and $(1, 1)$. The set $\{\text{pred}(\vec{v}), \text{succ}(\vec{v})\}$ is a set of keys of \vec{v} .*

4 Computing the appearance radius of a given vector

Thm. 1 will allow us to compute efficiently the appearance radius of any visible vector \vec{v} . The point is that we do not need to compute the test mask up to $R_{\text{app}}(\vec{v})$; we only need to test the inclusion of two balls — in direction $\text{pred}(\vec{v})$ and $\text{succ}(\vec{v})$.

We first examine the case of the vectors $(1, 0)$ and $(1, 1)$. It is easy to check that $\mathcal{T}(1) = \{(1, 0)\}$ and $\mathcal{T}(2) = \{(1, 0), (1, 1)\}$ (balls of radii 1 and 2 are drawn in Fig. 2):

- The smallest representable non-zero value for d_E^2 is 1. Since $p(1, 0)$ is in B_1 and does not belong to $\text{MA}(B_1)$ (the medial axis of a ball is its center), it follows that the appearance radius of $(1, 0)$ is 1.

- The next representable integer is 2. The point $q(1, 1)$ is not in $\text{MA}(B_2)$, however the point $(1, 0)$ does not forbid q from $\text{MA}(B_2)$ because $I_p(B_2)$ has radius 0. So $(1, 1)$ belongs to $\mathcal{T}(2)$.

We now proceed to the general case. For any visible vector \vec{v} in $G(\mathbb{Z}^2)$ different from $(1, 0)$ and $(1, 1)$, set $p = O + \vec{v}$, and let q and q' denote the predecessor and the successor of p . We know from Thm. 1 that the geometrical configuration for the appearance of \vec{v} is obtained for the smallest R for which $H_q(B_R) \not\subseteq H_p(B_R)$ and $H_{q'}(B_R) \not\subseteq H_p(B_R)$.

Alg. 1 works as follows: for all balls B_R in order of increasing radius R , it first computes $R_p = \mathcal{R}_p(B_R)$ and $R_q = \mathcal{R}_q(B_R)$ on line 4. The function $\text{Rcov}(R, \vec{z})$ computes, for any $R \geq 0$ and $\vec{z} \in \mathbb{Z}^2$, the covering radius of B_R in direction \vec{z} , that is to say, $\mathcal{R}_{O+\vec{z}}(B_R)$. Since $\vec{qp} = \vec{Oq'}$, we have $H_q(B_R) \not\subseteq H_p(B_R) \Leftrightarrow \text{Rcov}(R_q, \vec{Oq'}) > R_p$. So, if $\text{Rcov}(R_q, \vec{Oq'}) > R_p$, it remains to test whether $H_{q'}(B_R) \not\subseteq H_p(B_R)$; this is done in the same manner on line 6. In this case, i.e., if $\text{Rcov}(R_{q'}, \vec{Oq}) > R_p$ then neither q nor q' forbids O from $\text{MA}(B_p)$, hence $H_p(B_R)$ is a shape of smallest inner radius for which the inclusion test in direction \vec{Op} is mandatory. The existence of such a configuration is guaranteed by the fact that \vec{v} is visible [10].

Algorithm 1: Comp_Rapp

Input: a visible vector $\vec{v} = \vec{Op}$

Output: the appearance radius of \vec{v}

```

1 if  $\vec{v} = (1, 0)$  then return 1 ; if  $\vec{v} = (1, 1)$  then return 2 ;
2  $q \leftarrow \text{pred}(p)$  ;  $q' \leftarrow \text{succ}(p)$  ;  $R \leftarrow 0$  ;
3 loop
4    $R_p \leftarrow \text{Rcov}(R, \vec{v})$  ;  $R_q \leftarrow \text{Rcov}(R, \vec{Oq})$  ;
5   if  $\text{Rcov}(R_q, \vec{Oq'}) > R_p$  then
6      $R_{q'} \leftarrow \text{Rcov}(R, \vec{Oq'})$  ; if  $\text{Rcov}(R_{q'}, \vec{Oq}) > R_p$  then return  $R_p$  ;
7    $R \leftarrow R + 1$  ;
```

Let us examine the complexity of Alg. 1. First, the computation of $\vec{u} = \text{pred}(\vec{v})$ and $\vec{w} = \text{succ}(\vec{v})$ is easy: since $u_1v_2 - u_2v_1 = 1$, we are reduced to finding positive integers x and y satisfying $v_2x - v_1y = 1$. This can be achieved using the well-known extended Euclidean algorithm, in time $\mathcal{O}(\log(u_2))$.

The function $\text{Rcov}(R, \vec{v})$ consists in computing the maximum value of $\|\vec{Ox} + \vec{v}\|^2$ for all points x on the boundary of B_R . As R is the squared Euclidean radius of B_R , there are about \sqrt{R} points on the boundary of B_R . We use a simple Bresenham-Pitteway algorithm [13] to scan the boundary of B_R ; hence $\text{Rcov}(R, \vec{v})$ can be computed in time $\mathcal{O}(\sqrt{R})$.

Besides, the main loop is composed of at most 5 calls to Rcov with parameter R , thus the global complexity of the algorithm is roughly $\sum_{R=0}^{R_{app}(\vec{v})} \sqrt{R}$. We can find

a tight upper bound of this sum by using an integral: $\sum_{R=0}^S \sqrt{R} \leq \int_1^{S+1} \sqrt{R}$, which approaches $\frac{2}{3}S^{3/2}$ when $S \rightarrow \infty$. In consequence, Alg. 1 runs in time $\mathcal{O}(R_{app}^{3/2}(\vec{v})) = \mathcal{O}(r_{app}^3(\vec{v}))$. Furthermore, it is clear that this algorithm uses $\mathcal{O}(0)$ space.

5 An algorithm for $\mathcal{T}(R)$

In this section we propose an algorithm to compute $\mathcal{T}(R_{max})$ for any $R_{max} > 0$. This algorithm does not rely on the computation of DTs or LUTs, and need not scan the boundary of a ball when computing a covering radius. The basic idea is the following: we link each vector $\vec{v} \in G(\mathbb{Z}^2)$ to a vector $next(\vec{v}) \in G(\mathbb{Z}^2)$ whose norm is greater than or equal to that of \vec{v} (see Fig. 9) Thus, it is easy to localize the new points of a ball B_R , when R increases.

When invoked with parameter R_{max} , the algorithm is looking for the appearance configuration of all vectors \vec{v} whose norm are not greater than \sqrt{R} , for all representable integers R s.t. $R \leq R_{max}$. To do so, each visible vector also has three pointers $vecR(\vec{v})$, $testP(\vec{v})$ and $testS(\vec{v})$:

- $vecR(\vec{v})$ is a vector whose squared norm is equal to the radius of the largest open ball of center $O + \vec{v}$ included in B_R , i.e., the radius of $I_{O+\vec{v}}(B_R)$.
- $testP(\vec{v})$ (resp. $testS(\vec{v})$) is the vector $\vec{z} \in G(\mathbb{Z}^2)$ having minimum norm which satisfies $O + \vec{v} + \vec{z} \notin I_{O+pred(\vec{v})}(B_R)$ (resp. $\notin I_{O+succ(\vec{v})}(B_R)$).

The property $I_{O+\vec{v}}(B_R) \not\subseteq I_{O+pred(\vec{v})}(B_R)$ is therefore equivalent to $\|testP(\vec{v})\| \leq \|vecR(\vec{v})\|$. Similarly, $I_{O+\vec{v}}(B_R) \not\subseteq I_{O+succ(\vec{v})}(B_R) \Leftrightarrow \|testS(\vec{v})\| \leq \|vecR(\vec{v})\|$. See Fig. 9 and 10 for examples of links between vectors.

Let us give some details about Alg. 2. The vector $outV$ is the first vector in the linked list of vectors, whose norm is greater than \sqrt{R} . From line 5 to line 7, we update the list of vectors outside B_R (the grey points in Fig. 9 and 10): it is sufficient to insert the vector located above $outV$, and the vector on the right of $outV$ if its abscissa is 0. The new vectors must be inserted according to their norm. This is done by the procedure `insert_next`. When a new vector is inserted in the linked list, its pointers $vecR$, $testP$ and $testS$ are set to $(1, 0)$.

For each vector \vec{v} inside B_R , we update the pointers $vecR$ at lines 9 – 10, and we update the pointers $testP$ and $testS$ at lines 14 – 17. Then, the test of appearance of \vec{v} is done at line 18. Notice that for a given radius R , we need to scan the vectors \vec{v} in order of increasing norm (or, alternatively, in order of increasing abscissa) since the predecessor and successor of \vec{v} must both have their $vecR$ pointers updated.

Concerning the complexity of this algorithm: let us denote by $up(\vec{v}, R)$ the number of instructions required to update $vecR(\vec{v})$, $testP(\vec{v})$ and $testS(\vec{v})$ from R to the smallest representable integer greater than R . For each radius R , the time required to scan the vectors in B_R is roughly $\sum_{\|\vec{v}\|^2=1}^R up(\vec{v}, R)$; the procedure `insert_next` is negligible since it only has to scan the boundary of B_R

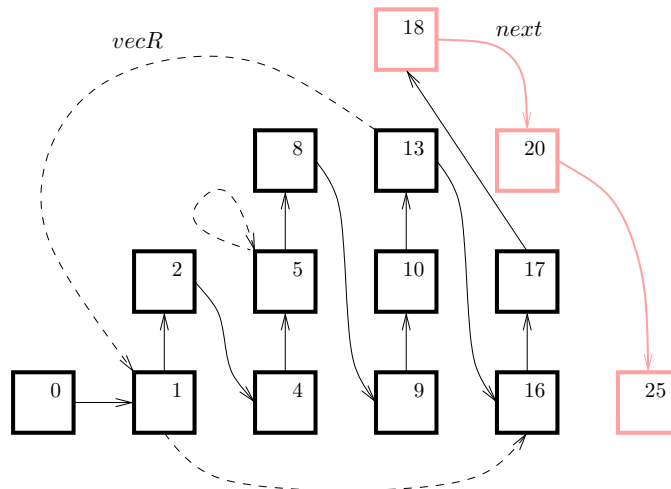


Fig. 9. Linked list of points inside the open ball B of radius 18 (black squares). Each point p has a pointer $next(p)$ to a point whose squared norm is the next representable integer (link represented by a solid arrow). The grey squares are the points of $G(\mathbb{Z}^2)$ on the outside of B , at the top of all columns around the boundary of B . The first grey point in the list gives the radius of the smallest ball strictly larger than B . Also, each visible point p has a pointer $vecR(p)$ (depicted by a dashed arrow) to the first point in the linked list whose squared norm is the radius of $I_p(B)$. For the sake of clarity, only 3 pointers $vecR$ are shown.

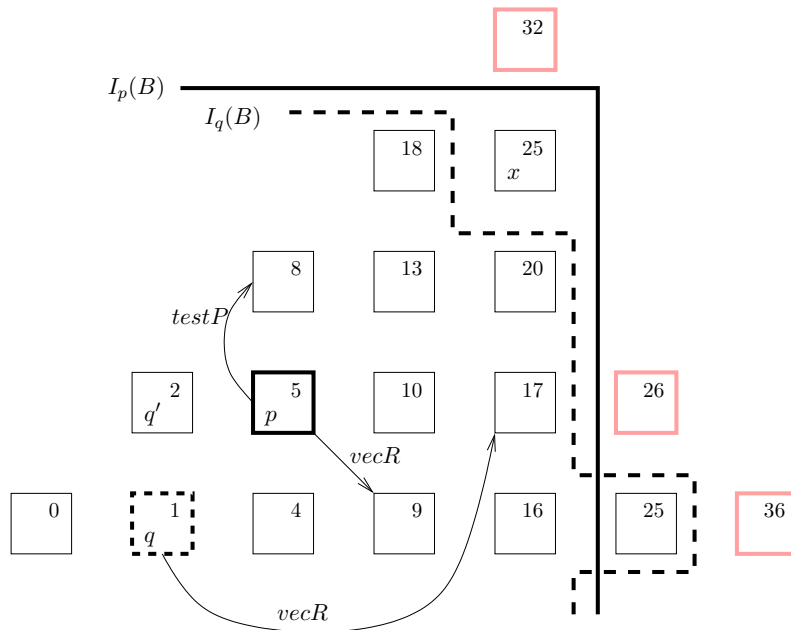


Fig. 10. Configuration for the open ball B of radius 26 (black squares). q is the predecessor of $p(2,1)$; $I_p(B)$ and $I_q(B)$ are open balls of respective radii 9 and 17. $testP(p) = \vec{px}$ is the smallest vector in $G(\mathbb{Z}^2)$ for which $x \notin I_q(B)$. Here $px < 9$, so $I_p(B) \not\subseteq I_q(B)$.

Algorithm 2: Comp_T

Input: a positive integer R_{max}
Output: the test mask $\mathcal{T}(R_{max})$, with the appearance radii of each vector

```

1  $T \leftarrow \{((1, 0), 1), ((1, 1), 2)\}$  ;
2  $outV \leftarrow Vector(2, 0)$  ;
3 while  $\|outV\|^2 \leq R_{max}$  do
4    $R \leftarrow \|outV\|^2$  ;
5   while  $\|outV\|^2 = R$  do
6      $insert\_next(outV)$  ;
7      $outV \leftarrow next(outV)$  ;
8   foreach visible vector  $v$  in  $B_R$ , in order of increasing norm do
9     while  $\|v + vecR(v)\|^2 \leq R$  do           /* update of  $vecR(v)$  */
10     $vecR(v) \leftarrow next(vecR(v))$  ;
11    if  $v \notin T$  then           /* update of  $testP(v)$  and  $testS(v)$  */
12       $u \leftarrow$  Farey predecessor of  $v$  ;
13       $w \leftarrow$  Farey successor of  $v$  ;
14      while  $\|w + testP(v)\| < \|vecR(u)\|$  do
15         $testP(v) \leftarrow next(testP(v))$  ;
16      while  $\|u + testS(v)\| < \|vecR(w)\|$  do
17         $testS(v) \leftarrow next(testS(v))$  ;
18      if  $\|testP(v)\| \leq \|vecR(v)\|$  and  $\|testS(v)\| \leq \|vecR(v)\|$  then
19         $T \leftarrow T \cup \{(v, R)\}$  ;           /* tests if  $v \in \mathcal{T}(R)$  */
20 return  $T$  ;
```

to insert new points. It follows that the global time complexity of the algorithm is roughly

$$\sum_{R=1}^{R_{max}} \sum_{\|\vec{v}\|^2=1}^R up(\vec{v}, R) \leq \sum_{R=1}^{R_{max}} \sum_{\|\vec{v}\|^2=1}^{R_{max}} up(\vec{v}, R) = \sum_{\|\vec{v}\|^2=1}^{R_{max}} \sum_{R=1}^{R_{max}} up(\vec{v}, R).$$

We now point out the fact that for any \vec{v} , the sum of the $up(\vec{v}, R)$ from $R = 1$ to R_{max} is $\mathcal{O}(R_{max})$, because the updates are done using a linked list. Hence, Alg. 2 runs in time

$$\mathcal{O}\left(\sum_{\|\vec{v}\|^2=1}^{R_{max}} R_{max}\right) = \mathcal{O}(R_{max}^2).$$

Besides, it is clear that this algorithm has space complexity linear in the number of points inside $B_{R_{max}}$, hence it runs in space $\mathcal{O}(R_{max})$.

6 Conclusion and experiments

We have established a link between the Farey sequences and covering relations between Euclidean disks. Accordingly, we have proposed two algorithms: the first

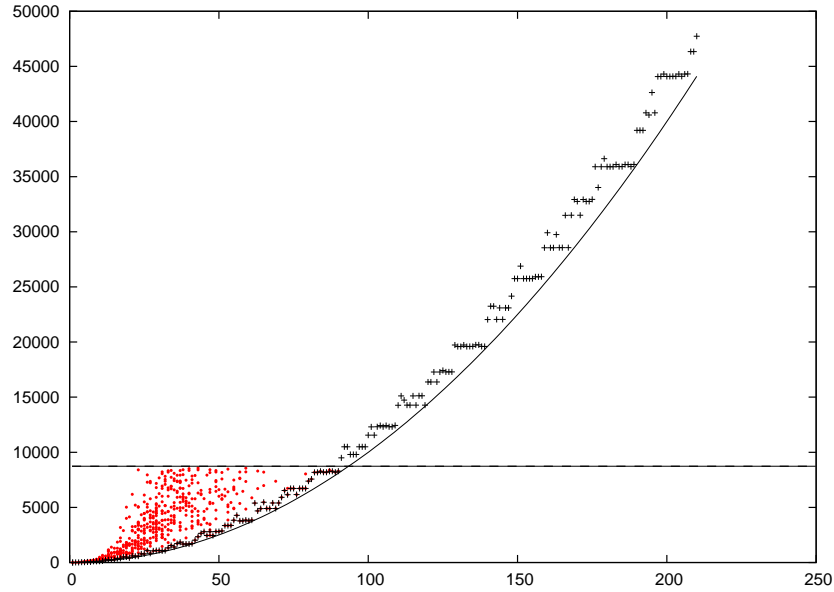


Fig. 11. Appearance radii of some visible vectors \vec{v} . Along the x-axis: abscissa v_1 of \vec{v} . Along the y-axis: $r_{app}(\vec{v})$, the Euclidean appearance radius of \vec{v} . The dots represent the 540 vectors of $\mathcal{T}(r = 8600)$; the crosses represent the vectors $(x, 1)$ for all $x \leq 210$. All the points we have found are above the function $y = x^2$.

one computes the appearance radius of any visible vector \vec{v} in time $\mathcal{O}(r_{app}^3(\vec{v}))$, the second one computes the test mask $\mathcal{T}(r)$ in time $\mathcal{O}(r^4)$.

The source code of our two algorithms is freely available in C language [14]. We illustrate outputs of these algorithms in Fig. 11. The dots in the bottom left corner have been computed by Alg. `Comp_T`; they represent the 540 vectors of $\mathcal{T}(r = 8600)$, which are necessary and sufficient to compute the medial axis of all the shapes that can be drawn within an image of size 17200×17200 pixels. In other words, we know all the vectors that are located below the dashed line (there is no vector in the bottom right corner). Prior to this, $\mathcal{T}(r)$ was known up to $r = 4800$ [7].

We have noticed that the vectors which are close to the x-axis, i.e., whose coordinates are $(x, 1)$ with $x \in \mathbb{N}_*$, have a small appearance radii compared to other vectors. So we used Alg. `Comp_Rapp` to compute the appearance radii of these vectors up to $x = 210$, see the crosses in Fig. 11. The results do not disprove the conjecture we expressed in [10], which suggests that the Euclidean appearance radius $r_{app}(\vec{v})$ of any visible vector $\vec{v} \in \mathbb{Z}^2$ is greater than the squared abscissa of \vec{v} . Moreover, these new data suggest that the bound is tight.

Also, we observed an interesting phenomenon: each time a vector \vec{v} appears in some $\mathcal{T}(r)$, we noticed that either the predecessor or the successor of \vec{v} had

already appeared. Furthermore, the smallest of these two vectors had appeared. We therefore conjecture the following: if \vec{v} belongs to some $\mathcal{T}(r)$, then the smallest vector among $\{\text{pred}(\vec{v}), \text{succ}(\vec{v})\}$ belongs to $\mathcal{T}(r)$.

Obviously, proving any of the above conjectures constitute a natural follow-up of this work, and would allow to speed up significantly the computation of the test mask.

References

1. Siddiqi, K., Pizer, S.M., Eds.: Medial Representations. *Comp. Imaging and Vision*, **37**, Springer, 2008.
2. Hirata, T.: A unified linear-time algorithm for computing distance maps. *Information Processing letters*, **58**(3):12–133, 1996.
3. Thiel, E.: Géométrie des distances de chanfrein. Habilitation à Diriger les Rech. Univ. de la Méditerranée, déc 2001. <http://www.lif.univ-mrs.fr/~thiel/hdr/>
4. Borgefors, G., Ragnemalm, I., and Sanniti di Baja, G.: The Euclidean DT, finding the local maxima and reconst. the shape. In 7th SCIA, 974–981, Aalborg, 1991.
5. Borgefors, G.: Centres of maximal disks in the 5-7-11 distance transform. In 8th SCIA, 105–111, Tromsø, 1993.
6. Rémy, E., Thiel, E.: Medial axis for chamfer distances: computing look-up tables and neighbourhoods in 2D or 3D. *Pattern Recog. Letters*, **23**(6):649–661, 2002.
7. Rémy, E., Thiel, E.: Exact Medial Axis with Euclidean Distance. *Image and Vision Computing*, **23**(2):167–175, 2005.
8. Normand, N., Évenou, P.: Medial axis LUT comp. for chamfer norms using H-polytopes. In: 14th DGCI, Lyon, France. LNCS **4992**:189–200, april 2008.
9. Normand, N., Évenou, P.: Medial axis lookup table and test neighborhood computation for 3D chamfer norms. *Pattern Recogn.*, 42(10):2288–2296, 2009.
10. Hulin, J., Thiel, E.: Visible vectors and discrete Euclidean medial axis. *Discrete and Computational Geometry*, in press, avail. online 10 dec. 2008.
11. Hulin, J., Thiel, E.: Appearance radii in medial axis test masks for small planar chamfer norms. In 15th DGCI, Discrete Geometry for Computer Imagery, LNCS **5810**:434–445, Montréal, Canada, Sept 2009.
12. Hardy, G.H., Wright, E.M.: An introduction to the theory of numbers. 5th edition, Oxford Science Pub., 1979.
13. Pitteway, M.L.V.: Algorithm for Drawing Ellipses or Hyperbolae with a Digital Plotter. *Computer J.*, **10**(3):282–289, 1967.
14. source code of the algorithms:
<http://pageperso.lif.univ-mrs.fr/~hulin/iwcia09/>